

Uncertainty relations for the Hohenberg-Kohn theorem

Purnima Ghale*

Cornell High Energy Synchrotron Source

Cornell University, Wilson Lab, Synchrotron Drive, Ithaca, NY, 14850

(Dated: April 28, 2022)

Abstract

How does charge density constrain many-body wavefunctions in nature? The Hohenberg-Kohn theorem for non-relativistic, interacting many-body Schrödinger systems is well-known and was proved using *reductio-ad-absurdum*; however, the physical mechanism or principle which enables this theorem in nature has not been understood. Here, we obtain effective canonical operators in the interacting many-body problem – (i) the local electric field, which mediates interaction between particles, and contributes to the potential energy; and (ii) the particle momenta, which contribute to the kinetic energy. The commutation of these operators results in the charge density distribution. Thus, quantum fluctuations of interacting many-particle systems are constrained by charge density, providing a mechanism by which an external potential, by coupling to the charge density, tunes the quantum-mechanical many-body wavefunction. As an initial test, we obtain the functional form for total energy of interacting many-particle systems, and in the uniform density limit, find promising agreement with Quantum Monte Carlo simulations.

The Hohenberg-Kohn theorem states that for non-relativistic many-electron systems described by the Schrödinger equation, once the external potential and charge density are fixed, the system is fully determined[1]. Specifically, we consider interacting many-body Schrödinger Hamiltonians in atomic units:

$$\hat{\mathcal{H}} = \underbrace{\sum_{\alpha} \frac{\hat{\mathbf{p}}_{\alpha}^2}{2}}_{\hat{T}} + \underbrace{\frac{1}{2} \sum_{\alpha \neq \beta} \frac{1}{|\hat{\mathbf{x}}_{\alpha} - \hat{\mathbf{x}}_{\beta}|}}_{\hat{V}_{ee}} + V_{ext}(\mathbf{r}) \quad (1a)$$

Let $\{\hat{\mathbf{x}}_{\alpha=1}, \dots, \hat{\mathbf{x}}_N\}$, $\{\hat{\mathbf{p}}_{\alpha=1}, \dots, \hat{\mathbf{p}}_N\}$, and $\{\mathbf{r}\}$ denote particle coordinates, particle momenta, and spatial coordinate on which local external potential $V_{ext}(\mathbf{r})$ is defined, respectively; \hat{T} and \hat{V}_{ee} denote kinetic and interaction energy operators, and many-body wavefunctions are denoted by $\Psi(\mathbf{x}_1, \dots, \mathbf{x}_N)$. The universal density functional, $F[n(\mathbf{r})]$, maps the complicated many-body wavefunction to a scalar field in three dimensions, and is defined by

$$F[n(\mathbf{r})] = \min_{\Psi \rightarrow n(\mathbf{r})} \left\{ \langle \Psi | \hat{T} + \hat{V}_{ee} | \Psi \rangle \right\} \quad (1b)$$

Mathematically, separate bounds on the kinetic energy, $\langle \Psi | \hat{T} | \Psi \rangle$, and the interaction energy, $\langle \Psi | \hat{V}_{ee} | \Psi \rangle$, have been obtained as functionals of charge density [2–5]. In addition, the Kohn-Sham ansatz[6, 7] can be used to understand weakly interacting systems with approximate exchange-correlation functionals, and a hierarchy of functionals of increasing complexity can be constructed[8–10]. But there are some limitations to prior work. One limitation is that constraints on the sum of operators, $\langle \Psi | \hat{T} + \hat{V}_{ee} | \Psi \rangle$, remain elusive. Another, is that not all particle densities correspond to quantum many-body ground states [11–13], and we cannot fully understand which densities are V -representable without direct mechanistic insight into $F[n(\mathbf{r})]$. Furthermore, while the Kohn-Sham ansatz[7] is highly effective, the non-factorizability of many-body wavefunctions [14] and ambiguity on the accuracy of exchange-correlation functionals[15–17], pose fundamental problems for quantum many-body systems with strong interactions. The benchmark calculations for many strongly-correlated systems are based on Quantum Monte Carlo (QMC)[18, 19], but even then, the number of possible fermion nodal surfaces or antisymmetric shapes of many-electron wavefunctions remains a challenge[20–23].

Despite difficulties in understanding interacting many-particle systems, however, the Hohenberg-

Kohn theorem is simple and universally applicable, shown via *reductio-ad-absurdum* in [1]. Our goal, therefore, is to understand the physical reason behind the success of this theorem – in particular, mechanistically, why/how does nature implement the Hohenberg-Kohn theorem?

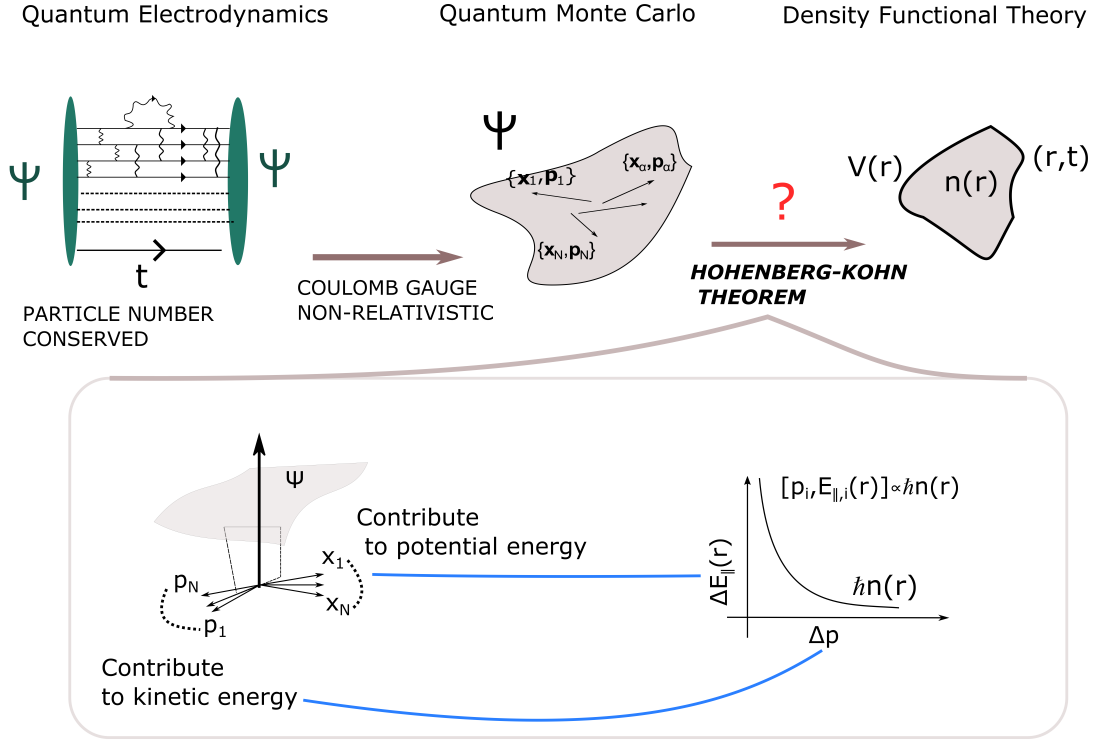


FIG. 1. In three conceptual leaps, relativistic particles dressed by photons can be investigated using a theory determined entirely in terms of charge density. Recall that longitudinal photons mediate interactions in Quantum Electrodynamics, and choosing the radiation gauge allows us to obtain the Quantum Monte Carlo Hamiltonian of Equation 1a. The Hohenberg-Kohn theorem then maps the many-body wavefunction Ψ to a scalar field $n(\mathbf{r})$, but the physical mechanism that enables this mapping was unknown. We propose the existence of effective canonical operators in interacting many-particle systems: particle momenta and local electric fields, with their commutation resulting in the local charge density. This operator algebra and the implied uncertainty relation constrain quantum fluctuations of interacting many-particle systems.

Figure 1 summarizes our main result. Longitudinal photons in radiation gauge of quantum electrodynamics correspond to the Coulomb interaction, $V_{ee} \sim \frac{1}{|\mathbf{x}_\alpha - \mathbf{x}_\beta|}$, of Equation 1a. $\langle \hat{V}_{ee} \rangle$ can therefore be replaced by the integrated energy density of the electric field. Moreover, we find that the local electric field and particle momentum are relevant canonical operators of the system: (i) these operators contribute to the potential and kinetic energy respectively, (ii) their quantum fluctuations contribute to the quantum-mechanical corrections to total

energy, and (iii) commutation of the two operators results in the charge density, such that charge density constrains quantum fluctuations of the many-body system. We will first derive the relationship between operators shown in Figure 1, and use that relation to obtain a functional form for total energy of interacting many-particle systems. For the jellium model, the functional form obtained in this way agrees with reference Quantum Monte Carlo (QMC) simulations.

Interaction energy in terms of longitudinal electric fields – We first show that the electron-electron interaction is the square of the energy density of the electric field:

$$\langle \Psi | \hat{V}_{ee} | \Psi \rangle = \frac{1}{8\pi} \int_{\mathbf{r}} \langle \Psi | \hat{\mathbf{E}}_{\parallel}(\mathbf{r}) \cdot \hat{\mathbf{E}}_{\parallel}(\mathbf{r}) | \Psi \rangle \quad (2)$$

where $\hat{\mathbf{E}}_{\parallel}(\mathbf{r})$ denotes the electric field generated by particles with coordinates $\{\mathbf{x}_1, \dots, \mathbf{x}_{\alpha}, \dots, \mathbf{x}_N\}$ at point \mathbf{r} , and is given by the gradient of the local potential $\hat{\mathbf{E}}_{\parallel,j}(\mathbf{r}) = -\partial_{r_j} \sum_{\beta} \frac{1}{|\mathbf{r} - \mathbf{x}_{\beta}|}$. Let us now consider:

$$\int_r \langle \Psi | \hat{\mathbf{E}}_{\parallel}(\mathbf{r}) \cdot \hat{\mathbf{E}}_{\parallel}(\mathbf{r}) | \Psi \rangle = \int_r \langle \Psi | \sum_{\alpha,\beta} \partial_{r_j} \frac{1}{|\mathbf{r} - \mathbf{x}_{\alpha}|} \cdot \partial_{r_j} \frac{1}{|\mathbf{r} - \mathbf{x}_{\beta}|} | \Psi \rangle \quad (3a)$$

Integrating by parts in \mathbf{r} , and setting surface terms to zero, we obtain

$$= - \sum_{\alpha,\beta} \int_r \langle \Psi | \frac{1}{|\mathbf{r} - \mathbf{x}_{\alpha}|} \nabla_r^2 \frac{1}{|\mathbf{r} - \mathbf{x}_{\beta}|} | \Psi \rangle \quad (3b)$$

Using $\nabla_r^2 \frac{1}{|\mathbf{r} - \mathbf{x}_{\beta}|} = -4\pi\delta^{(3)}(\mathbf{r} - \mathbf{x}_{\beta})$, results in

$$= \sum_{\alpha,\beta} \int_r \langle \Psi | \frac{4\pi}{|\mathbf{r} - \mathbf{x}_{\alpha}|} \delta^{(3)}(\mathbf{r} - \mathbf{x}_{\beta}) | \Psi \rangle = 4\pi \sum_{\alpha,\beta} \langle \Psi | \frac{1}{|\mathbf{x}_{\beta} - \mathbf{x}_{\alpha}|} | \Psi \rangle \quad (3c)$$

$$= 4\pi \sum_{\alpha \neq \beta} \langle \Psi | \frac{1}{|\mathbf{x}_{\beta} - \mathbf{x}_{\alpha}|} | \Psi \rangle + 4\pi N \underbrace{\langle \Psi | \int_r \frac{\delta(\mathbf{r} - \mathbf{x}_1)}{|\mathbf{r} - \mathbf{x}_1|} | \Psi \rangle}_{\Lambda} \quad (3d)$$

The last term, denoting self-interaction, simplifies to a renormalizable constant, $(\sqrt{2\pi})^3 \int_{\mathbf{k}} \frac{1}{|\mathbf{k}|^2} \rightarrow \Lambda$ and depends on the UV-cutoff used for regularization, alternatively, also see [24]. We

have thus obtained the interaction energy in terms of longitudinal electric fields, as follows.

$$\int_r \langle \Psi | \hat{\mathbf{E}}_{\parallel}(\mathbf{r}) \cdot \hat{\mathbf{E}}_{\parallel}(\mathbf{r}) | \Psi \rangle = 8\pi \langle \Psi | \hat{V}_{ee} | \Psi \rangle + 4\pi N\Lambda \quad (3e)$$

A similar analysis (integration by parts, setting surface terms to zero, and using $\nabla_r^2 \frac{1}{|\mathbf{r}-\mathbf{x}|} = \delta^{(3)}(\mathbf{r}-\mathbf{x})$) results in the connection between the energy density of the classically defined electric field, and the electrostatic interaction between charges, as follows.

$$\int_r \langle \Psi | \hat{\mathbf{E}}_{\parallel}(\mathbf{r}) | \Psi \rangle \cdot \langle \Psi | \hat{\mathbf{E}}_{\parallel}(\mathbf{r}) | \Psi \rangle = 8\pi \int_{r,r'} \frac{1}{2} \frac{n(\mathbf{r})n(\mathbf{r}')}{|\mathbf{r}-\mathbf{r}'|} \quad (4)$$

Using Eqs 3e and 4, the interaction energy, $\langle \Psi | \hat{V}_{ee} | \Psi \rangle$, separates into a classical, electrostatic contribution, and contributions due to quantum fluctuations of $\hat{\mathbf{E}}_{\parallel}(\mathbf{r})$.

$$\langle \hat{V}_{ee} \rangle = \frac{1}{8\pi} \langle \hat{\mathbf{E}}_{\parallel}(\mathbf{r}) \rangle \cdot \langle \hat{\mathbf{E}}_{\parallel}(\mathbf{r}) \rangle + \frac{1}{8\pi} \int_r \Delta \mathbf{E}_{\parallel}^2(\mathbf{r}) \quad (5)$$

$$\langle \hat{V}_{ee} \rangle = \frac{1}{2} \int_{r,r'} \frac{n(\mathbf{r})n(\mathbf{r}')}{|\mathbf{r}-\mathbf{r}'|} + \frac{1}{8\pi} \int_r \Delta \mathbf{E}_{\parallel}^2(\mathbf{r}) \quad (6)$$

where $\Delta \mathbf{E}_{\parallel}^2(\mathbf{r}) = \langle \hat{\mathbf{E}}_{\parallel}(\mathbf{r}) \cdot \hat{\mathbf{E}}_{\parallel}(\mathbf{r}) \rangle - \langle \hat{\mathbf{E}}_{\parallel}(\mathbf{r}) \rangle \cdot \langle \hat{\mathbf{E}}_{\parallel}(\mathbf{r}) \rangle$.

Kinetic energy of many-particle quantum systems – As for contributions to kinetic energy, let us assume for convenience that the total momentum, $\langle \hat{\mathbf{p}} \rangle = 0$, i.e. the many-particle system is not undergoing translation, or the reference frame is chosen to be so. Particle indistinguishability then implies[25, see p. 320] $\langle \hat{\mathbf{p}}_{1,i} \rangle = \langle \hat{\mathbf{p}}_{2,i} \rangle = \dots = \langle \hat{\mathbf{p}}_{N,i} \rangle = 0$, and the kinetic energy is the sum of fluctuations of momentum,

$$\langle \hat{T} \rangle = \sum_{\alpha=1}^N \frac{\Delta \mathbf{p}_{\alpha}^2}{2} \quad (7)$$

where $\Delta \mathbf{p}_{\alpha}^2 = \langle \hat{\mathbf{p}}_{\alpha}^2 \rangle - \langle \hat{\mathbf{p}}_{\alpha} \rangle^2$. The universal interacting many-body functional, $F[n(\mathbf{r})]$, in terms of classical electrostatic energy and quantum fluctuations is

$$F[n(\mathbf{r})] = \langle \hat{T} + \hat{V}_{ee} \rangle = \sum_{\alpha} \frac{\Delta \mathbf{p}_{\alpha}^2}{2} + \frac{1}{2} \int_{r,r'} \frac{n(\mathbf{r})n(\mathbf{r}')}{|\mathbf{r}-\mathbf{r}'|} + \frac{1}{8\pi} \int_r \Delta \mathbf{E}_{\parallel}^2(\mathbf{r}) \quad (8)$$

Effective commutation relation – We have thus mapped the many-body Schrödinger hamiltonian to classical and quantum contributions, such that the quantum contributions are given by

$$\mathcal{E}_{quantum} = \sum_{\alpha} \frac{\Delta \mathbf{p}_{\alpha}^2}{2} + \frac{1}{8\pi} \int_{\mathbf{r}} \Delta \mathbf{E}_{\parallel}^2(\mathbf{r}) \quad (9a)$$

Inspecting the relationship between the momentum and electric field operators via commutation, we obtain

$$[\hat{\mathbf{p}}_{j,\alpha}, \hat{\mathbf{E}}_{\parallel,k}(\mathbf{r})]\Psi = \frac{\hbar}{i} (\partial_{x_{j,\alpha}} \mathbf{E}_{\parallel,k}(\mathbf{r})) \Psi = -\frac{\hbar}{i} \left(\partial_{x_{j,\alpha}} \partial_{r_k} \sum_{\beta} \frac{1}{|\mathbf{r} - \mathbf{x}_{\beta}|} \right) \Psi \quad (9b)$$

Changing the order of differentiation, $\partial_{x_{j,\alpha}}$ selects only $\alpha = \beta$ from summation over β ; furthermore, $\partial_{x_j} \frac{1}{|\mathbf{r} - \mathbf{x}|} = \partial_{r_j} \frac{1}{|\mathbf{r} - \mathbf{x}|}$. Thus, we obtain:

$$[\hat{\mathbf{p}}_{j,\alpha}, \hat{\mathbf{E}}_{\parallel,k}(\mathbf{r})]\Psi = \frac{\hbar}{i} \left(-\partial_{r_j} \partial_{r_k} \frac{1}{|\mathbf{r} - \mathbf{x}_{\alpha}|} \right) \Psi \quad (9c)$$

Using $j = k$ terms, summation over repeated indices, and $-\nabla_r^2 \frac{1}{|\mathbf{r} - \mathbf{x}|} = 4\pi\delta^{(3)}(\mathbf{r} - \mathbf{x})$, we obtain:

$$[\hat{\mathbf{p}}_{j,\alpha}, \hat{\mathbf{E}}_{\parallel,j}(\mathbf{r})]\Psi = \frac{\hbar}{i} \left(-\nabla_r^2 \frac{1}{|\mathbf{r} - \mathbf{x}_{\alpha}|} \right) \Psi = \frac{4\pi\hbar}{i} \delta^{(3)}(\mathbf{r} - \mathbf{x}_{\alpha}) \quad (9d)$$

Summation over particle labels, α gives:

$$\sum_{\alpha} [\hat{\mathbf{p}}_{\alpha,j}, \hat{\mathbf{E}}_{\parallel,j}(\mathbf{r})]\Psi = \frac{4\pi\hbar}{i} \hat{n}(\mathbf{r}) \quad (9e)$$

From particle indistinguishability, we obtain:

$$N[\hat{\mathbf{p}}_j, \hat{\mathbf{E}}_{\parallel,j}(\mathbf{r})]\Psi = \frac{4\pi\hbar}{i} \hat{n}(\mathbf{r}) \quad (9f)$$

Constraint on quantum fluctuations of canonical variables – Let us now constrain quantum fluctuations. Applying the Cauchy-Schwartz inequality following Robertson[26], the commutation relations in Equation 9c imply the following relation between quantum fluctuations:

$$\Delta \mathbf{p}_{j,\alpha} \Delta \mathbf{E}_{\parallel,k} \geq \frac{\hbar}{2} \left| \langle \Psi | -\partial_{r_j} \partial_{r_k} \frac{1}{|\mathbf{r} - \mathbf{x}_{\alpha}|} | \Psi \rangle \right| \quad (10a)$$

Using $|g(x)| \geq g(x)$, summing over three dimensions, and using the Poisson relation between potential and charge density, again, leads to

$$\Delta \mathbf{p}_{j,\alpha} \Delta \mathbf{E}_{\parallel,j}(\mathbf{r}) \geq 2\pi\hbar \langle \hat{n}_\alpha(\mathbf{r}) \rangle \quad (10b)$$

Summation over particle labels, assuming isotropy of fluctuations,

$$\Delta \mathbf{p}_x^2 = \Delta \mathbf{p}_y^2 = \Delta \mathbf{p}_z^2 = \Delta p^2 \quad (10c)$$

$$\Delta \mathbf{E}_{\parallel,x}^2(\mathbf{r}) = \Delta \mathbf{E}_{\parallel,y}^2(\mathbf{r}) = \Delta \mathbf{E}_{\parallel,z}^2(\mathbf{r}) = \Delta E_{\parallel}^2(\mathbf{r}) \quad (10d)$$

and using particle indistinguishability, we get

$$3N\Delta p\Delta E_{\parallel}(\mathbf{r}) \geq 2\pi\hbar n(\mathbf{r}) \quad (10e)$$

Equation 10e suggests that by fixing $n(\mathbf{r})$, we are essentially realizing a generalized uncertainty constraint on quantum fluctuations of the many-particle system. Note that we are constraining fluctuations of longitudinal photons, which on their own have negative normalization in field theory [27]. It is therefore better to leave the inequality indeterminate for now as follows.

$$3N\Delta p\Delta E_{\parallel}(\mathbf{r}) \sim 2\pi\hbar n(\mathbf{r}) \quad (10f)$$

Effect of uncertainty relation on energy as a functional of $n(\mathbf{r})$ – Equation 10f will now be used to obtain a density functional expression for total energies of many-body quantum states. In particular, the kinetic energy is constrained by charge density as $\langle \hat{T} \rangle \geq C_{ke} \int_{\mathbf{r}} n^{5/3}(\mathbf{r})$ [28]. Using the fact that $\langle \hat{T} \rangle$ is due to momentum fluctuations only, see Eq 7, we obtain

$$\langle T \rangle = 3N\Delta p^2/2 \geq C_{ke} \int_{\mathbf{r}} n^{5/3}(\mathbf{r}) \quad (11a)$$

Instead of this bound, one could also obtain momentum fluctuations using (trial) Kohn-Sham wavefunctions, and improve bounds on momentum fluctuations iteratively. Also note that the constant C_{ke} depends on the (anti)symmetry and spin-degeneracy of the system[29][30]. With momentum fluctuations available, we can now use Equation 10f, to constrain fluctu-

ations of the electric field, and making that substitution, we obtain the total energy as a functional of $n(\mathbf{r})$ as follows [31]

$$\mathcal{E}[n(\mathbf{r})] \sim C_{ke} \int n^{5/3}(\mathbf{r}) + \frac{\pi}{2C_{ke}N} \int \frac{n^2}{n^{5/3}} + \frac{1}{2} \int \frac{n(\mathbf{r})n(\mathbf{r}')}{|\mathbf{r} - \mathbf{r}'|} + \int V_{ext}(\mathbf{r})n(\mathbf{r}) \quad (11b)$$

Energy in the uniform density limit – In the uniform density limit, $n(\mathbf{r}) = n$ and $V_{ext}(\mathbf{r}) = -\int_{\mathbf{r}'} \frac{n}{|\mathbf{r} - \mathbf{r}'|}$, a uniform positively charged background. The total energy then is:

$$\mathcal{E}[n(\mathbf{r})] \sim C_{ke}n^{5/3}\mathcal{V} + \frac{\pi}{2C_{ke}N} \frac{n^2\mathcal{V}}{n^{5/3}} + \frac{n^2}{2} \int \frac{1}{|\mathbf{r} - \mathbf{r}'|} d^3\mathbf{r}d^3\mathbf{r}' - n^2 \int \frac{1}{|\mathbf{r} - \mathbf{r}'|} d^3\mathbf{r}d^3\mathbf{r}' \quad (11c)$$

where \mathcal{V} denotes volume of the system; let us use $n\mathcal{V} = N$ to substitute \mathcal{V} in the first term on the *right-hand-side*. Then, in terms of the Wigner-Seitz radius, $\frac{4\pi}{3}r_s^3 = \frac{1}{n}$, the energy is given by

$$\mathcal{E}^{uniform}[n] \sim NC_{ke} \left(\frac{3}{4\pi r_s^3} \right)^{2/3} + \frac{\pi}{2NC_{ke}} \left(\frac{3}{4\pi r_s^3} \right)^{1/3} + A(\mathcal{V})/2 \left(\frac{3}{4\pi r_s^3} \right)^2 + c_1(N) \quad (11d)$$

where we have added a constant term, $c_1(N)$ independent of r_s , but dependent on the total number of particles, N (note the self-interaction constant that we ignored earlier). Rearranging in decreasing powers of r_s , we get:

$$\mathcal{E}^{uniform}[n(\mathbf{r})] \sim c_1(N) + c_2(N) \frac{1}{r_s} + c_3(N) \frac{1}{r_s^2} + c_4(\mathcal{V}) \frac{1}{r_s^6} \quad (11e)$$

How “universal” is the energy expression in the uniform density limit? – Equation 11e shows that bosonic and fermionic systems share the same r_s dependencies despite (anti)symmetry or spin-degeneracy of Ψ . By linearity, we expect energy-differences between states that satisfy Equation 11e to also satisfy the same r_s dependencies. Let us now fit Equation 11e against reference values of energies and energy-differences of different quantum states investigated using Quantum Monte Carlo[19].

Figure 2 shows the agreement of the functional form in Equation 11e to four types of quantum many-body states: bosonic fluid (BF), paramagnetic fermionic fluid (PMF), ferromagnetic fermion fluid (FMF), and Wigner crystalline state (BCC). Specifically, Figure 2 presents

| | | | |
|--|----------|----------|----------|
| Coefficients for Eq. 11e: | | | |
| {-0.0041, -1.2336, 0.7985, -2.0181} {-0.0039, -1.2624, 2.5656, -0.1254} {-0.0034, -1.3089, 3.5297, 1.7527} {-0.0043, -1.2026, 0.8972, 0} | | | |
| Maximum Absolute Errors: | | | |
| 1.43 mHa | 1.36 mHa | 1.26 mHa | 1.14 mHa |

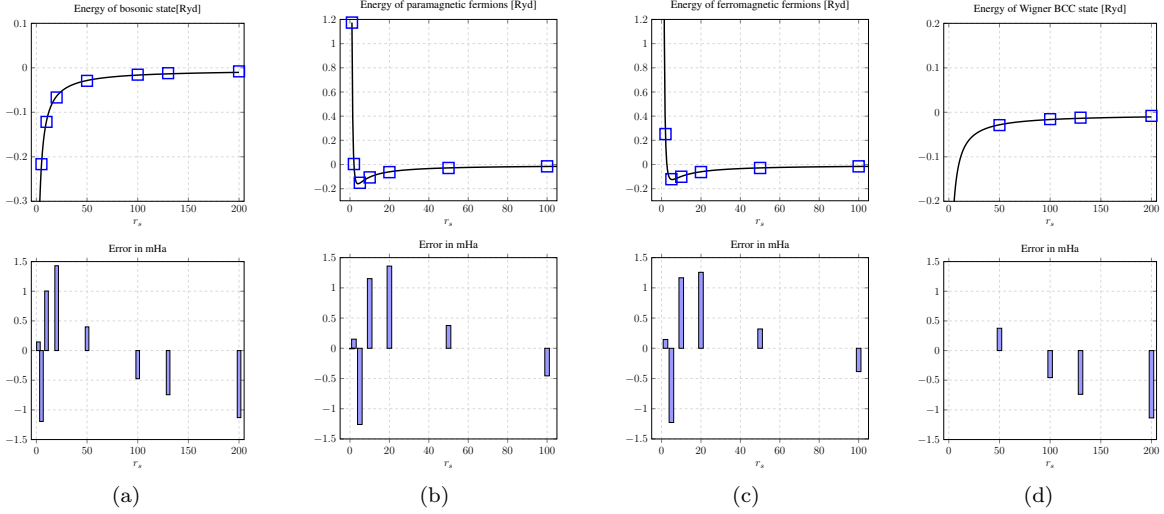


FIG. 2. Consistency of Equation 11e with Quantum Monte Carlo calculations of four types of many-body quantum wavefunctions in the uniform density limit [19]: (a) bosonic Ψ (b) paramagnetic fermion (c) ferromagnetic fermion and (d) the Wigner BCC state. The first and second rows show coefficients obtained via semi-empirical fits of Equation 11e, and corresponding maximum absolute deviation from QMC reference data in [19]. The third row shows energy as a function of r_s where parameterized forms of Equation 11e (solid lines) agree with QMC data (discrete points). Finally, deviation of energies from reference QMC data is plotted throughout the range of available data. Note that energies are in Ryd = 0.5Ha in keeping with [19], and deviations are within ± 1.5 mHa. These results support the general forms of r_s dependence arising from uncertainty arguments in the previous section.

the coefficients that best describe each many-body quantum state, the maximum absolute deviation from reference data, comparison plots of energies (and deviations) of the functional form from QMC data for the complete range of r_s values. Agreement of the functional form in Eq. 11e to reference values within ± 1.5 mHa suggests that we have captured the most essential physics implied by the kinetic and potential energy operators – despite differences in the particle statistics, spin polarization, and crystallinity of different wavefunctions, they are described by the Hamiltonian (and resulting operator algebra) in Equation 1a.

How well can we arrange many-body states by energy? – We now consider whether Equation 11e is capable of representing transitions between quantum states. Energy-differences appear to generally agree with the r_s dependencies, with notable exception around change in spin-polarization.

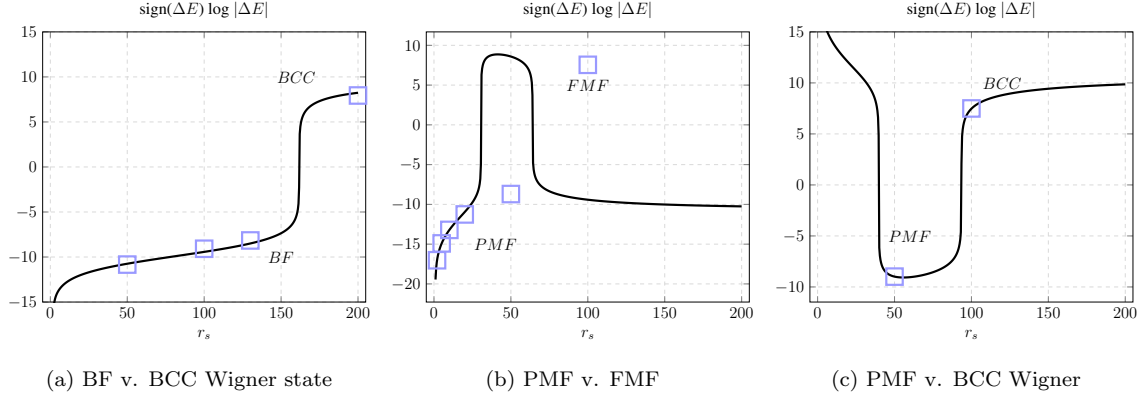


FIG. 3. Energetic ordering of different quantum states in the jellium model, with discrete points showing QMC data[19], and solid lines showing fits to Equation 11e, with coefficients from Figure 2. Transitions occur when energy-differences change sign at $y = 0$, with energetically favored states labeled before and after transition: (a) Transition between Bosonic fluid (BF) to BCC Wigner state is captured exactly at $r_s = 160$, (b) Transition between paramagnetic fermions (PMF) and ferromagnetic fermions (FMF) is not captured accurately, and (c) Transition between paramagnetic fermions (PMF) to BCC Wigner state is captured, despite the lack of reference datapoints [19]. As expected, the functional form does not capture spin-orbit coupling, absent in the Hamiltonian, while accurately representing the competition between kinetic and interaction energies that drive transitions around the Wigner state. Data from other QMC simulations are not combined, as each QMC simulation assumes extensivity, Jastrow factors, and sampling heuristics, with subtle effects that are beyond the scope of this work.

Figure 3 shows energy differences between pairs of states. Specifically, in Figure 3a, the bosonic fluid (BF) to Wigner (BCC) state transition is captured exactly at $r_s = 160$, in agreement with [19], while in Figure 3b, the functional form is unable to capture energy differences (and the transition) between paramagnetic and ferromagnetic states, despite high accuracy in energy prediction (*cf.* Fig. 2). This disagreement is promising (and expected) because while we have captured the competition between kinetic and interaction energies in the system, spin-orbit coupling, which crucial to determine the paramagnetic-to-ferromagnetic transition is not included. Finally, in Figure 3c, we observe that despite the lack of datapoints, the transition between Wigner (BCC) and paramagnetic fermion (PMF) states is correctly captured, as it is driven by competition between kinetic and interaction energies. More data from other sources are not used to complement the reference dataset in [19], as each Quantum Monte Carlo simulation assumes size-extensivity, sampling heuristics, and trial wavefunctions that can lead to subtle effects, for instance see [32].

Conclusion In this work, we have illuminated the pivotal role of the underlying electro-

magnetic field in the Hohenberg-Kohn theorem. It is shown that we can construct effective canonical variables for interacting many-body Hamiltonians, obtain uncertainty relations, and understand mechanistically, how nature implements the Hohenberg-Kohn theorem. Semi-empirical fits to QMC simulations in the uniform density limit agree with our conceptual proposal, but more work is necessary to develop universal density functionals based on the insights of this work, to conduct universality tests on benchmark non-uniform systems, and to handle periodicity.

We can now understand the Hamiltonian in Equation 1a in terms of quantum fluctuations; one can similarly understand electron-phonon interactions in terms of quantum fluctuations of the external potential; understanding spin-orbit coupling and quantum magnetism, however, remains a challenge. More work along this direction would enable us to make general, material-agnostic, statements about the connection between antiferromagnetism and quantum phases such as strange-metals, high-temperature superconductors, and other non-fermi liquids[14].

Acknowledgements This material is based in part upon work supported by the Department of Energy, National Nuclear Security Administration, under Award Number DE-NA0002374, in collaboration with Prof. Harley T. Johnson at the University of Illinois. Discussions with Johnson, David Ceperley, Andre Schleife and Lucas Wagner at University of Illinois are all gratefully acknowledged. This work is also based in part upon research conducted at the Center for High Energy X-ray Sciences (CHEXS) which is supported by the National Science Foundation under award DMR-1829070. Discussions with Jacob Ruff at the Cornell High Energy Synchrotron Source (CHESS) are gratefully acknowledged.

* pg472@cornell.edu

- [1] Pierre Hohenberg and Walter Kohn. Inhomogeneous electron gas. *Physical Review*, 136(3B):B864, 1964.
- [2] Garnet Kin-Lic Chan and Nicholas C Handy. Optimized Lieb-Oxford bound for the exchange-correlation energy. *Physical Review A*, 59(4):3075, 1999.
- [3] Elliott H Lieb. A lower bound for Coulomb energies. *Physics Letters A*, 70(5-6):444–446,

1979.

- [4] Elliott H Lieb and Stephen Oxford. Improved lower bound on the indirect coulomb energy. *International Journal of Quantum Chemistry*, 19(3):427–439, 1981.
- [5] Elliott H. Lieb and Walter E. Thirring. Bound for the kinetic energy of fermions which proves the stability of matter. *Physical Review Letters*, 35:687–689, Sep 1975.
- [6] LJ Sham and Walter Kohn. One-particle properties of an inhomogeneous interacting electron gas. *Physical Review*, 145(2):561, 1966.
- [7] Walter Kohn and Lu Jeu Sham. Self-consistent equations including exchange and correlation effects. *Physical Review*, 140(4A):A1133, 1965.
- [8] John P Perdew and Karla Schmidt. Jacob’s ladder of density functional approximations for the exchange-correlation energy. In *AIP Conference Proceedings*, volume 577, pages 1–20. AIP, 2001.
- [9] Narbe Mardirossian and Martin Head-Gordon. Mapping the genome of meta-generalized gradient approximation density functionals: The search for B97M-V. *The Journal of Chemical Physics*, 142(7):074111, 2015.
- [10] Jianmin Tao, John P Perdew, Viktor N Staroverov, and Gustavo E Scuseria. Climbing the density functional ladder: Nonempirical meta-generalized gradient approximation designed for molecules and solids. *Physical Review Letters*, 91(14):146401, 2003.
- [11] Walter Kohn. V-representability and density functional theory. *Physical Review Letters*, 51(17):1596, 1983.
- [12] Weitao Yang, Paul W Ayers, and Qin Wu. Potential functionals: dual to density functionals and solution to the v-representability problem. *Physical Review Letters*, 92(14):146404, 2004.
- [13] Elliott H Lieb. Density Functionals for Coulomb Systems. *International Journal of Quantum Chemistry*, 24:243, 1983.
- [14] Sung-Sik Lee. Recent developments in non-fermi liquid theory. *Annual Review of Condensed Matter Physics*, 9(1):227–244, 2018.
- [15] Michael G. Medvedev, Ivan S. Bushmarinov, Jianwei Sun, John P. Perdew, and Konstantin A. Lyssenko. Density functional theory is straying from the path toward the exact functional. *Science*, 355(6320):49–52, 2017.
- [16] Sharon Hammes-Schiffer. A conundrum for density functional theory. *Science*, 355(6320):28–29, 2017.

- [17] Kasper P. Kepp. Comment on “Density functional theory is straying from the path toward the exact functional”. *Science*, 356(6337):496–496, 2017.
- [18] David M Ceperley. Ground state of the fermion one-component plasma: A Monte Carlo study in two and three dimensions. *Physical Review B*, 18(7):3126, 1978.
- [19] David M Ceperley and BJ Alder. Ground state of the electron gas by a stochastic method. *Physical Review Letters*, 45(7):566, 1980.
- [20] Lubos Mitas. Structure of fermion nodes and nodal cells. *Physical Review Letters*, 96(24):240402, 2006.
- [21] David M Ceperley. Fermion nodes. *Journal of Statistical Physics*, 63(5-6):1237–1267, 1991.
- [22] J Carlson, Stefano Gandolfi, Kevin E Schmidt, and Shiwei Zhang. Auxiliary-field quantum monte carlo method for strongly paired fermions. *Physical Review A*, 84(6):061602, 2011.
- [23] DK Sunko. Natural generalization of the ground-state slater determinant to more than one dimension. *Physical Review A*, 93(6):062109, 2016.
- [24] Use $\int \frac{1}{|\mathbf{k}|^2} d^3\mathbf{k} = \lim_{m \rightarrow 0} \int \frac{1}{k^2 + m^2} d^3\mathbf{k}$. In D dimensions, the integral is generalized to

$$\begin{aligned}
I(D) &= \int \frac{d^D k}{(2\pi)^D} \frac{1}{\mathbf{k}^2 + m^2} \\
&= \frac{2\pi}{(2\pi)^D} \prod_{k=1}^{D-2} \int_0^\pi \sin^k \theta_k d\theta_k \int_0^\infty dk k^{D-1} \frac{1}{k^2 + m^2} \\
&= \frac{S_D}{(2\pi)^D} \int_0^\infty dk k^{D-1} \frac{1}{k^2 + m^2}
\end{aligned}$$

where $S_D = \frac{2\pi^{D/2}}{\Gamma(D/2)}$ is the surface of a unit sphere in D dimensions. Substituting $k^2 = ym^2$, the resulting integral can be written as : $B(\alpha, \gamma) = \frac{\Gamma(\alpha)\Gamma(\gamma)}{\Gamma(\alpha+\gamma)} = \int_0^\infty dy y^{\alpha-1} (1+y)^{-\alpha-\gamma}$ We find that:

$$\lim_{m \rightarrow 0} I(D) = \frac{(m^2)^{D/2-1}}{(4\pi)^{D/2}} \Gamma(1 - D/2) = 0$$

- [25] Elliott H Lieb. Kinetic energy bounds and their application to the stability of matter. In *Inequalities, Selecta of Elliot H Lieb, Eds. Loss and Ruskai*, pages 317–328. Springer, 2002.
- [26] Howard Percy Robertson. The uncertainty principle. *Physical Review*, 34(1):163, 1929.
- [27] Lewis H Ryder. *Quantum field theory*. Cambridge university press, 1996.
- [28] Elliott H. Lieb and Walter E. Thirring. Bound for the kinetic energy of fermions which proves the stability of matter. *Phys. Rev. Lett.*, 35:687–689, Sep 1975.

- [29] Elliott H Lieb and Walter E Thirring. Inequalities for the moments of the eigenvalues of the Schrodinger Hamiltonian and their relation to Sobolev inequalities. In *The Stability of Matter: From Atoms to Stars*, pages 135–169. Springer, 1991.
- [30] Specifically, the C_{ke} for a bosonic system varies by a factor $\propto N^{-2/3}$ from that of a fermionic system.
- [31] Could we have used constraints on $\langle V_{ee} \rangle$ [2, 4] first, and then applied Equation 10e to constrain momentum fluctuations? This approach is not as fruitful: bounds on $\langle \hat{V}_{ee} \rangle$ do not distinguish between fermionic and bosonic systems [33]; more importantly, bounds on $\langle V_{ee} \rangle$ do not contain local information necessary to constrain $\Delta E_{\parallel}^2(\mathbf{r})$.
- [32] RJ Needs, MD Towler, ND Drummond, Pablo Lopez Rios, and JR Trail. Variational and diffusion quantum monte carlo calculations with the casino code. *The Journal of Chemical Physics*, 152(15):154106, 2020.
- [33] Here we elaborate on previous Lieb-Thirring and Lieb-Oxford type bounds on kinetic and interaction energies respectively, where the effect of antisymmetry is somewhat tangentially discussed. Suppose we have a many-body solution for interacting systems with distinguishable particle labels, $\Psi_C(x_1, \dots, x_N)$, that results in a charge density, $n(\mathbf{r})$. One can construct a symmetric (bosonic) many-body wavefunction, Ψ_S , by summing over permutations of the coordinate labels,

$$\Psi_S(x_1, \dots, x_N) = \frac{1}{\sqrt{N!}} \sum_{\mathcal{P}(x_1, \dots, x_N)} \Psi(\mathcal{P})$$

To obtain a corresponding antisymmetric (fermionic) many-body wavefunction resulting in the same charge density, $n(\mathbf{r})$, Ψ_A , we multiply the symmetric wavefunction by $\Theta(x_1, \dots, x_N)$, where $\Theta = \pm 1$ represents the fermion nodal structure and changes sign under exchange of coordinate labels, $\Psi_A = \Theta(x_1, \dots, x_N) \Psi_S(x_1, \dots, x_N)$. In the following, subscripts S denote observables of symmetric wavefunctions while A denote observables corresponding to anti-symmetric wavefunctions. We find that expectation values of operators like $\delta(\mathbf{r} - x_\alpha)$, and $\frac{1}{|x_\alpha - x_\beta|}$ remain unchanged because for antisymmetric wavefunctions, the integrals simply include $\Theta^2 = 1$:

$$n_A(\mathbf{r}) = \int_{x_1, \dots, x_N} |\Psi_A|^2 \delta(\mathbf{r} - x_\alpha) = \int_{x_1, \dots, x_N} |\Psi_S|^2 \delta(\mathbf{r} - x_\alpha) \Theta^2 = n_S(\mathbf{r})$$

$$V_{ee,A}(\mathbf{r}) = \int_{x_1, \dots, x_N} |\Psi_A|^2 \frac{1}{|x_\alpha - x_\beta|} = \int_{x_1, \dots, x_N} |\Psi_S|^2 \frac{1}{|x_\alpha - x_\beta|} \Theta^2 = V_{ee,S}(\mathbf{r})$$

On the other hand, the momentum operator requires the derivative of Ψ , and the presence of nodal structure becomes relevant. Specifically, for $\Psi_S \rightarrow \Psi_A$ related by the fermion nodal structure, the observed momenta vary because:

$$\langle p \rangle_{\alpha,A} = \frac{\hbar}{i} \int_{x_1, \dots, x_N} \Psi_A^\dagger(x_1, \dots, x_N) \nabla_\alpha \Psi_A(x_1, \dots, x_N)$$

Operating the derivative on $\nabla_\alpha \Psi_A = (\nabla_\alpha \Psi_S) \Theta + \Psi_S \nabla_\alpha \Theta$, resulting in

$$\langle p \rangle_{\alpha,A} = \langle p \rangle_{\alpha,S} + \frac{\hbar}{i} \int_{x_1, \dots, x_N} |\Psi_S|^2 \Theta(x_1, \dots, x_N) \nabla_\alpha \Theta(x_1, \dots, x_N)$$

In case of the local electric field operator, the gradient is with respect to \mathbf{r} acting on $\frac{1}{|\mathbf{r}-\mathbf{x}_1|} \Psi(x_1, \dots, x_N)$, and derivatives on the nodal-surface do not appear.